LA-UR-08-06524

Improving a Turning Process Using Piezoelectric Actuators

Peter P. Radecki[1], Walter A. Kruse[2], Aaron J. Welsh[3], Erik A. Moro[4],
Gyuhae Park[4], Matthew T. Bement[4]

[1] Dept. of Mechanical Engineering, Michigan Technological University
[2] Dept. of Mechanical Engineering, New Mexico Institute of Mining and Technology
[3] Dept. of Materials Science and Engineering, Pennsylvania State University
[4] The Engineering Institute, Los Alamos National Laboratory, Los Alamos, NM 87545

ABSTRACT

An adaptive vibration control technique for improving surface finish is explored. In some cases, additional processing to improve surface finish quality after machining, such as grinding or polishing, is either not feasible or is not cost-effective. The focus of this research is on the development of an improved turning processes through the use of active vibration damping. Demonstration of the tool holder shows reduced relative tool-workpiece vibration and improved surface finish. The toolholder employs a high bandwidth piezoelectric actuator and collocated piezoelectric displacement sensor, with an adaptive positive position feedback control algorithm for vibration control and chatter reduction. The performance of this method is evaluated by comparing the surface finishes obtained with active vibration control versus baseline uncontrolled cuts. Surface finish roughness was measured using profilometry gages. Considerable improvement in surface finish and reduction in chatter amplitude are observed analyzed for applications in modern day machining.

1 INTRODUCTION

1.1 Background

Historically the manufacturing of parts with precision finishes has been broken into separate processes: first machining is performed with mills or lathes to create overall shapes and then grinding and polishing is performed to create the desired surface finish.

Traditionally surface finish smoothness beyond 100 μm cannot be achieved with machining. Machining removes material from a workpiece by shearing off material from the surface, forming a chip. Continuous chips that are a stable thickness and well attached produce a good surface finish by keeping cutting forces constant. However, discontinuous chip formation causes changes in cutting forces which can cause vibration in the tool tip. This leaves valleys, pits, and deposits in the workpiece which adversely affect surface finish. To compound this problem, materials are never perfectly structured. Grain boundaries and impurities can also cause discontinuous chip formation and change cutting forces which can lead to chatter [1].

Chatter, unwanted vibration between the tool and workpiece, is a primary cause of surface finish roughness. Chatter occurs when forces in the cutting process cause relative motion between the tool tip and the workpiece. This is manifested when the tool tip and workpiece start bouncing off of each other and leave visible unwanted surface finish defects, commonly known as chatter marks. If the toolholder or workpiece are not stiff enough to support the machining forces, then chatter will occur. Chatter often limits the depth for boring operations and the depth of cut and feed rates for turning and facing operations. Traditionally chatter reduction is accomplished by stiffening boring bars and toolholders, using sharper cutters, supporting workpieces with a follower or tailstock, or even providing damping to

the workpiece by attaching vibration reduction materials such as rubber to an area on the workpiece which is not being machined. Because chatter can be amplified by machining at resonant frequencies or the tool or workpiece, or from forced vibration from within the machine, sometimes chatter reduction is achieved by reducing the spindle speed, changing the feed rate, or reducing the depth of cut. However, for particularly hard materials and processes which have high tolerances for surface finish or very precise dimensional tolerances, these measures may not be enough to reduce chatter to an acceptable level [1].

An alternative, modern way to reduce chatter is by actively detecting and suppressing the unwanted vibration with a control algorithm and an actuator which uses active materials. Active materials are materials that exhibit a coupling between two or more of their physical properties. Piezoelectrics, for example, experience an elastic strain when exposed to an electric field and are excellent candidates for vibration control because they can be driven at high frequencies with high force by electrical signals. Recent research has demonstrated the effectiveness of using active material actuators for chatter reduction [2].

1.2 Previous Work

The use of active materials for non-conventional machining techniques has been studied extensively in recent years. For example, active materials have been used to drive fast tool servos (FTS) for use in ultraprecision machining operations such as diamond turning. A FTS serves as an auxiliary actuator for positioning the cutting tool with high bandwidth and excellent positional accuracy [2]. As an example, researchers at North Carolina State University developed an FTS which could correct for thermally induced position errors with high accuracy and improve surface finish. Other researchers have reported similar results, achieving positional accuracies as high as 10 nm [2].

Ultrasonic-assisted machining (UAM), where high-frequency, low-amplitude vibrations are induced at the tool tip during cutting, also uses active materials as actuators. UAM has also seen considerable development, particularly for use in machining hard, brittle materials such as superalloys, ceramics, certain composites and glass. Babitsky et. al. studied the effects of ultrasonically assisted turning on high strength nickel-based alloys, and found a substantial improvement in both surface roughness and dimensional accuracy [32]. In addition to turning, UAM has been successfully applied to other machining processes. For example, Chang and Bone demonstrated that ultrasonic drilling at the proper frequency changes cutting dynamics, which reduces the thrust force and burr size in a typical drilling operation [4]. Because of its potential for improving existing machining processes, researchers have developed analytical models of UAM processes to study thermal effects and relationships between UAM parameters and performance characteristics [5,6].

In machining processes, chatter reduction is the primary application for adaptive vibration control. A variety of different control techniques have been studied for use in the application, including regenerative feedback [8], wave-based control [9], and positive position feedback (PPF) [2]. Piezoelectric-driven adaptive vibration suppression systems have been shown to substantially improve stability in turning operations as well as in other machining operations such as boring and milling [2].

1.3 Applications of Adaptive Vibration Control

Machining a smooth surface finish without additional processing could have applications across diverse manufacturing areas. Specifically at Los Alamos National Laboratory (LANL), machining plutonium with high quality surface finish is required for weapons manufacturing. The high cost of plutonium

along with its toxicity makes a high precision manufacturing operation with a single setup on a CNC lathe more cost effective. Outside of weapons manufacturing, Park et. al. explain how vibration controlled machining techniques can be used to improve surface finish with low cost machine tools [2]. With further research and development, active vibration control could possibly be applied to mature industries, such as automotive engine components provided the process is cost efficient and reliable.

2 EXPERIMENTAL PROCEDURE

2.1 Project Overview

This project focuses on chatter reduction through active vibration control. The toolholder characterized in this study uses a collocated piezoelectric actuator and sensor for active vibration control. The adaptive vibration control toolholder, shown in Figure 1, was developed at LANL and was characterized by Espinoza et al. [10]. The collocated piezoelectric stack eliminates the need for an external sensor. This holder will be driven by an adaptive positive position feedback controller and will be used for vibration suppression and chatter reduction. Because plutonium is extremely expensive and dangerous, aluminum will be used as a reasonable substitute because of its similar ductility and general material properties. Visual inspection and non-contact profilometry of the workpiece will be used to measure the surface finish quality for characterizing the effectiveness of each toolholder.

Figure 1: Adaptive Vibration Control Toolholder with piezoelectric actuator/sensor

2.2 Adaptive Vibration Control Toolholder Development

An adaptive positive position feedback (PPF) controller was used to drive the actuator for the vibration reduction toolholder. This form of controller was chosen because it has been used successfully in vibration reduction applications and because it can be used with frequency tracking algorithms to dynamically adapt to changes in the system such as varying mass and stiffness that occur during a machining operation. PPF control dynamically damps vibration by moving in phase with the vibration to neutralize relative motion. This equalizes workpiece-cutting interaction forces, reducing vibration amplitude and force. This is easily conceived for a basic turning operation on bar-stock with a long length to diameter ratio (length/diameter > 3). The workpiece has more torsional rigidity than bending rigidity so if cutting inconsistencies occur, the workpiece starts bouncing off the cutting blade. Moving the cutting blade in phase with this vibration causes the relative forces and motion to decrease,

improving surface finish quality and eliminating chatter.

Development and tuning of this adaptive PPF controller was tested and experimented first on a cantilever beam, secondly with the toolholder sitting on a benchtop and finally with the toolholder mounted on a lathe with turning and facing operations.

Figure 3 shows a schematic of an adaptive PPF controller for our application. The PPF controller is driven by a transfer function in Equation 1 where g is the gain of the transfer function, ω_f is the filter frequency, and ξ_f is the filter damping ratio [11]:

$$K(s) = \frac{g\omega_f^2}{s^2 + 2\xi_f \omega_f s + \omega_f^2}. \tag{1}$$

The adaptive portion of the controller tracks the resonant frequency of the structure and dynamically tunes its transfer function to this frequency. In Figure 3 this is shown as a Fast Fourier Transform (FFT). Essentially the FFT picks out the first resonant frequency in a specified range of the structure and sets ω_f in the transfer function to this new value.

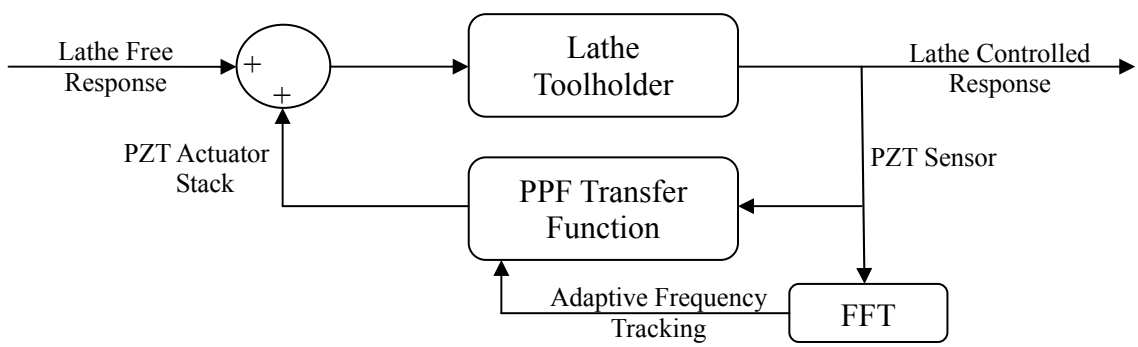

Figure 3: Adaptive Positive Position Feedback Control

Initial control algorithm and hardware testing was performed on a simple cantilever beam comprised of two piezoelectric sheets attached to a rectangular polycarbonate bar, as shown in Figure 4. This beam allowed for visual inspection of controller performance and easy tuning of the PPF controller. The beam was controlled with a Simulink model of our control algorithm, which was ported to an xPC Target real-time system as shown in Figure 5. A National Instruments DAC system and 200 volt inverting amplifier were used to control the actuator and measure the beam response from the sensor. The piezoelectric patch on the left in Figure 4 was the sensor and the while the larger patch on the right was the actuator.

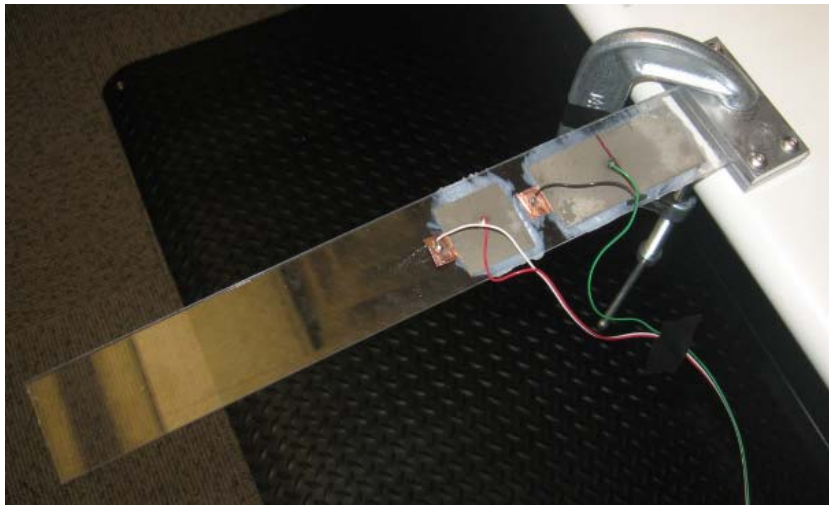

Figure 4: Low-power test beam.

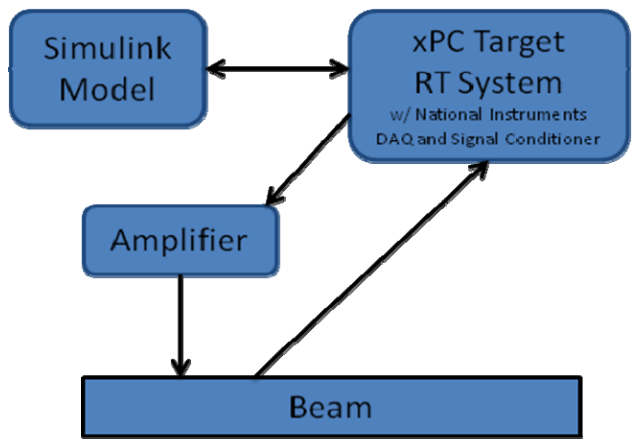

Figure 5: Experimental setup for static PPF and adaptive PPF control tests.

The beam was excited by plucking the free end a fixed displacement and allowing it to vibrate freely. The controller was tuned by comparing the uncontrolled response with the PPF controlled response while adjusting the controller gain, damping ratio and filtering frequency to obtain optimum performance. The resonant frequency of the first bending mode of the beam was measured using a DACTRON Photon data acquisition board and the RT Pro modal analysis software, which performed an FFT on the time response data. The measured resonant frequency, ω_n , was 6 Hz. Standard rules of thumb for initial PPF tuning are to set the controller's gain g=1, damping ratio ξ_{PPF} =10*$\xi_{free_response}$ and filter frequency ω_{PPF} =(0.75 to 1.4)*ω_n. Testing yielded optimum performance with values of g=1.5, ξ_f =0.4 and ω_f = 0.9*ω_n for our controller. These tests showed significant improvements in damping performance over natural damping while maintaining stability. For this initial tuning test the transfer function *K(s)* was implemented as a continuous transfer function in the s-domain. Simulink digitized the controller in the background when porting the model to xPC Target.

The adaptive portion of the controller is driven by an FFT algorithm so the transfer function is updated at a slower frequency than the controller's sampling frequency. This frequency difference exists because both the FFT and transfer function are receiving the same digitized time response signal from

the sensor but the FFT requires several (specifically some power of two) subsequent time-signal data points in order to perform an FFT. The transfer function is only updated after the FFT algorithm is run on the buffered data set. Implementing a self-updating control algorithm in Simulink requires modeling the controller transfer function discretely. The controller was digitized by performing a z-transform on the continuous transfer function *K(s)*. Tustin's approximation, shown in Equation (2), was used for finding the discrete-domain form of the Laplace-domain PPF controller function [12].

$$s = \frac{2}{T}\frac{(z-1)}{(z+1)} \tag{2}$$

T is the sampling period of the control system. The z-domain transfer function shown in Equation (3) was calculated by substituting Equation (2) into Equation (1).

$$H(z) = \frac{\left(\frac{\omega_f^2}{d}\right)z^2 + \left(\frac{2\omega_f^2}{d}\right)z + \left(\frac{\omega_f^2}{d}\right)}{z^2 + \left(\frac{\frac{-8}{T^2} + 2\omega_f^2}{d}\right)z + \left(\frac{\frac{4}{T^2} - \frac{4\xi_f\omega_f}{T} + \omega_f^2}{d}\right)} \tag{3}$$

$$d = \frac{4}{T^2} + \frac{4\xi_f\omega_f}{T} + \omega_f^2$$

After digitization of the controller, beam response tests were run to check the new model for stability and compare the performance of both models. Figure 6 shows controlled response from both the continuous and discrete versions of the PPF controller. This proved the controller was stable and ready to have the adaptive self-tuning algorithm implemented.

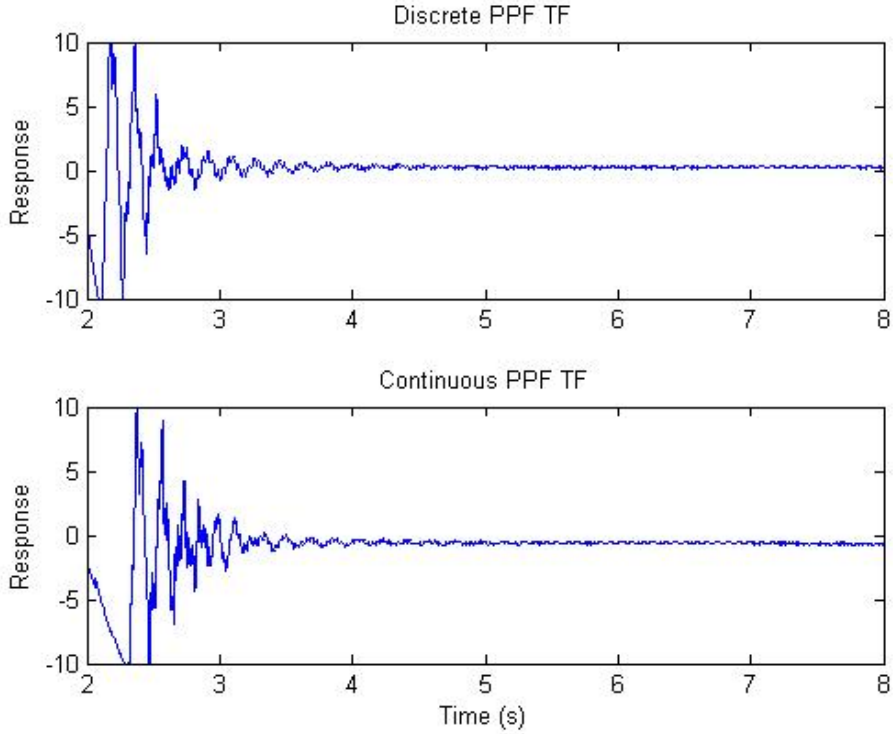

Figure 6: System response for PPF control. (Top) Discrete transfer function. (Bottom) Continuous transfer function.

The adaptive portion of the controller in Simulink was implemented by taking the FFT of the input signal, writing a custom script to detect the first resonant mode in frequency domain from the FFT, and then dynamically updating the control transfer function with the new frequency. To ensure controller stability for the beam, the maximum filter frequency change between subsequent FFT runs was set at 10% of the previous frequency. The performance of the adaptive controller was tested by changing the mass of the beam by taping a large washer to the free end. The non-adaptive discrete controller was tuned to operate at 6 Hz (the natural frequency of the polycarbonate beam without additional mass). With the added mass, the beam's natural frequency decreased to 3 Hz, a 50% change. The adaptive vibration controller showed an improvement over the non-adaptive case by demonstrating its ability to dynamically tune itself. Figure 7 shows the performance improvement of the adaptive version of the controller over the non-adaptive controller and a baseline uncontrolled case.

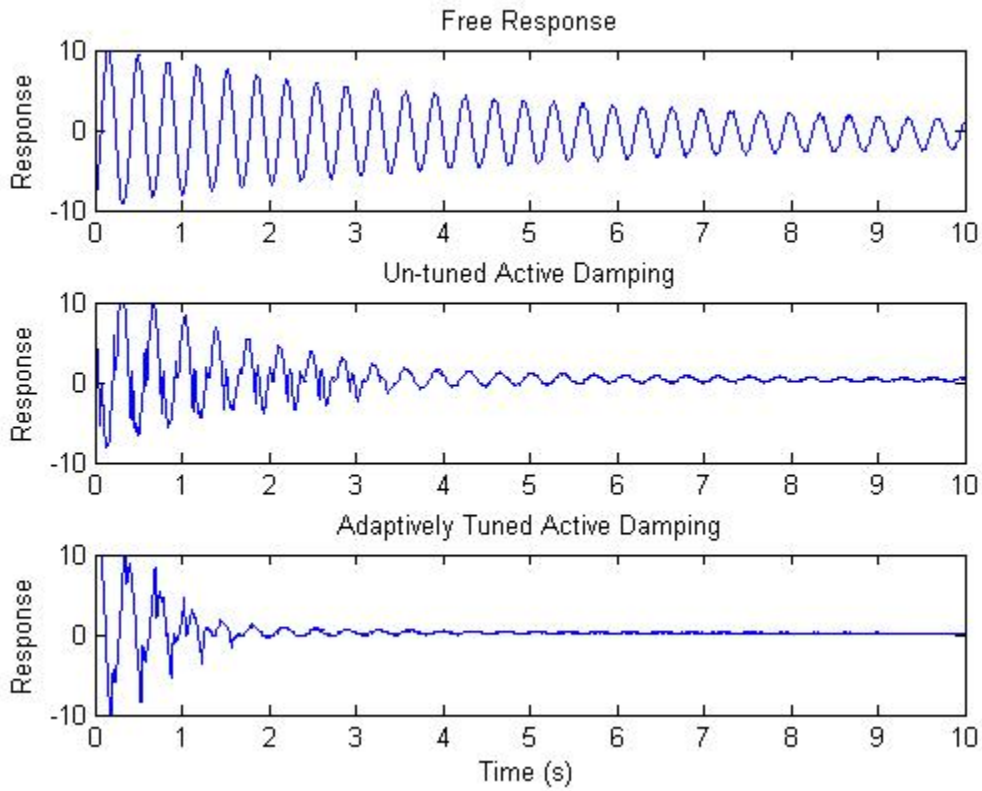

Figure 7. System response for Adaptive PPF control with added mass. (Top) Free vibration case. (Center) Static PPF control tuned to 6 Hz. (Bottom) Adaptive PPF control.

Damping ratios, estimated using log-decrement calculations on the time responses from Figure 4 and 5, appear in Table 1. These damping ratios provide a quantitative comparison of discrete versus continuous transfer function and adaptive versus non-adaptive controller for two performance defining test cases. Comparing these ratios, it can be seen that there is no significant difference between the continuous and discrete-form transfer functions in static PPF control, and that the adaptive system provides a substantial improvement over non-adaptive control when the system mass or stiffness is perturbed.

Table 1. Estimated damping ratios for low-power control experiments.

Test	1st Bending Mode	Damping Ratio
Free vibration	6 Hz	3.6%
PPF control tuned at 6 Hz, continuous TF		9.0%
PPF control tuned at 6 Hz, discrete TF		9.9%
Free vibration	3 Hz	1.2%
Static PPF control tuned at 6 Hz		3.2%
Adaptive PPF control		7.4%

The toolholder was tested with the same hardware setup; the actuator was simply swapped in for the beam. For the beam testing, the sampling frequency of the controller was over two orders of magnitude higher than the bending mode that the filter was targeting. For the toolholder there wasn't such a large margin. An FFT of the toolholder performed with the Dactron and RT Pro showed the first bending mode to be around 3.7 kHz. The Pentium 4 processor which was running the xPC Target control platform overloaded at an execution frequency around 18.5kHz meaning that the controller was

sampling much closer to the target filter frequency. This caused Tustin's approximation of the z-tranform to go unstable because the transformation maps the frequency range $-\infty < \omega_f < +\infty$ to $-\pi / T < \omega_d < +\pi / T$ where T is the sampling period. For filter frequencies close to zero, this distortion is minimal, but for a target frequency that is a quarter of the sampling frequency, this will cause the controller to be mistuned and possibly go unstable. Frequency pre-warping was used to correct for this. Equation (4) shows the pre-warping that was applied to ω_f to correct for this instability [12].

$$\varpi_d = \frac{2}{T} \tan(\omega_f \frac{T}{2}) \tag{4}$$

Testing the vibration reduction toolholder was done first by exciting the tip of the cutting blade with an impact hammer and inspecting the time response of the holder as measured from the collocated piezoelectric sensor while the control algorithm damped out vibration with the piezoelectric actuator. Tuning the controller for the tool holder was similar to tuning the controller for the beam. Further testing of the toolholder was done by applying random noise to the actuator. The free and controlled responses from this test were analyzed in the frequency domain by running an FFT on the time signals. The first bending mode of the vibration response was reduced effectively with the same transfer function constants that were applied during the impact analysis. Unfortunately the amplitude of the higher frequency response was increased because of spillover from the PPF controller. Additional PPF filters were applied to those higher frequency modes to damp them out but this just caused even higher frequency spillover around the Nyquist frequency which could not be tuned out reliably with additional PPF filters. Alternatively a low pass filter was added to the first mode PPF filter. This low pass filter reduced almost all of the high frequency spillover without reducing the performance of the PPF controller. With this design, about 10 dB of amplitude reduction occurred across the first resonant mode of the toolholder, as shown in Figure 8. This single adaptive PPF coupled with a low pass filter was used as the controller for the lathe testing.

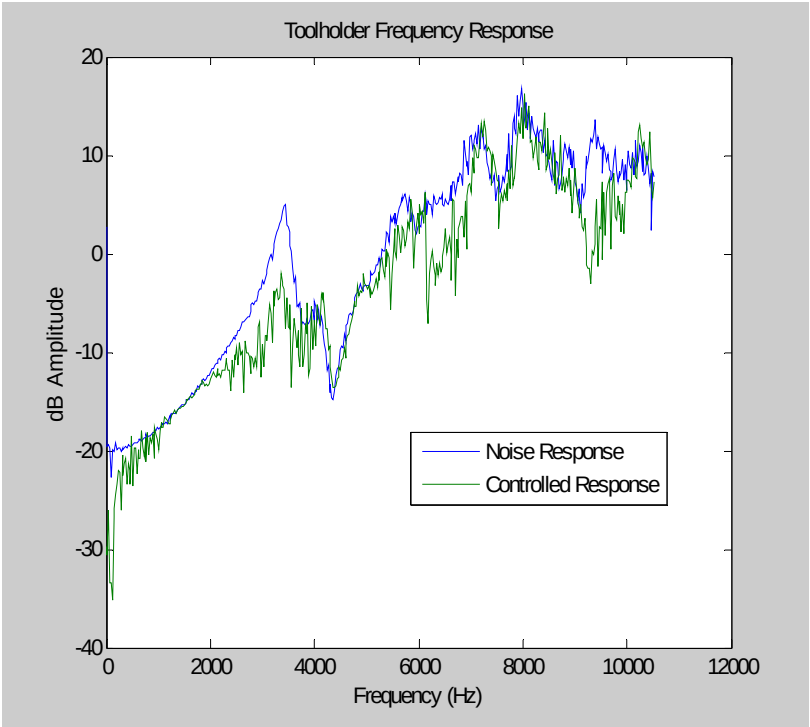

Figure 8: Bending Mode Amplitude Reduction

2.3 Experimental Procedure

Testing was done on two different lathe setups. The facing tests were done with a Pneumo Precision T-Base lathe, while turning tests were done on a traditional manual lathe. Uncontrolled test specimens were cut with the toolholder electronics turned off. Then electronics were turned on and further tests were run while adjusting PPF constants such as gain, damping ratio, and frequency multiplier for the vibration reduction toolholder to improve performance. Live performance inspection was done by running an FFT of the sensor time signal and comparing the magnitudes of the response against the baseline response with the electronics turned off. The first resonance in this FFT is expected to have the largest magnitude because it has the lowest frequency and therefore the largest impact on chatter. This frequency is dependent on the lathe configuration, workpiece material, cutting speeds and cutting blade parameters and is not well documented or predictable. In order to compensate for this, the first resonance frequency from uncontrolled baseline test will be used to seed the adaptive PPF controller. Tool wear was assumed to be negligible because of the low hardness of the workpiece material and the relatively slow cutting speeds, so the insert was not changed between cuts.

The facing setup consisted of vacuum fixturing a 13 inch diameter disc of high purity aluminum and cutting half inch radial facing cuts. The spindle was set for constant cutting speed so that the cutting blade would be in uniform cutting conditions throughout the facing operation. This setup was tested with the adaptive vibration control toolholder and can be seen in Figure 9. Besides the uncontrolled and controlled tests, sine wave and sine sweep tests were done in the 3 to 4 kHz range for comparison. Samples were measured using non-contact profilometry, and average surface roughness values were obtained for each of the half inch bands.

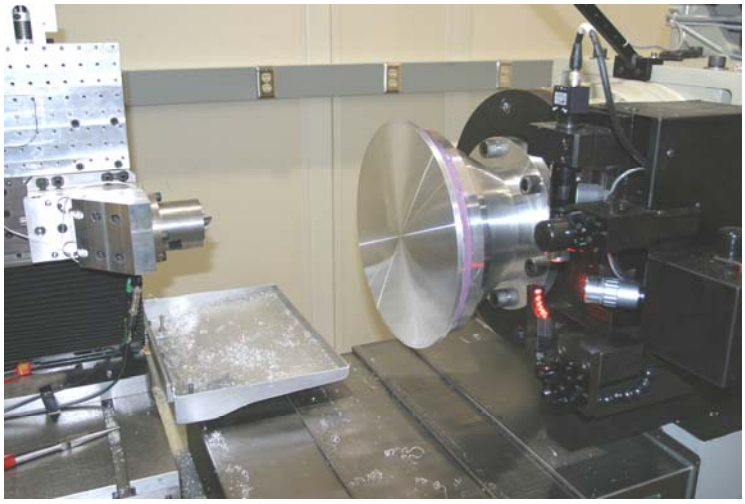

Figure 9: Pneumo Precision T-Base Lathe

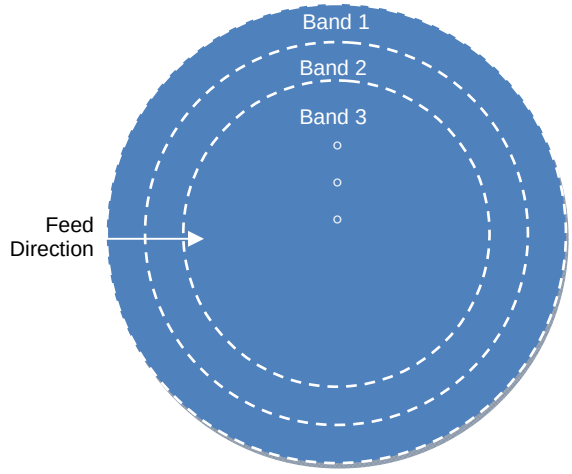

Figure 10: Facing Bands

The turning setup consisted of using Aluminum 6061 T6 bar stock mounted in a 3 jaw chuck on a shop-floor Kent USA manual lathe. Turning was done on the free end of bar stock where the length to diameter ratio was greater than three. Cutting parameters were set so that visible chatter was induced. Several cuts were done with different cutting control parameters for the adaptive controller. Contact surface profilometry was recorded after each turning pass to compare surface finishes.

3 RESULTS AND ANALYSIS

Facing cuts were the first tests performed and yielded bad results. The uncontrolled test showed that the resonant peak during a lathe operation shifted downwards compared to the benchtop tests from 3700 Hz to 2800 Hz. Analysis of frequency response data showed increased amplitude of vibration at the first resonant peak with both the adaptive and non-adaptive version of the PPF controller compared to uncontrolled tests. Surface profilometry data showed no noticeable improvement from the controlled versus the uncontrolled baseline tests regardless of how the PPF controller was tuned.

The lathe used for the facing cuts was an industrial high precision lathe and the workpiece on the lathe was extremely well supported so there was little room for chatter to occur. We hypothesized that running tests with more chatter present in the uncontrolled case would give the PPF controller a better chance to performe positively.

Turning tests on the manual lathe were done next with a bar stock that exhibited chatter when turned at 1200 rpm. The primary resonant frequency occurred at 515 Hz. Unfortunately tuning the control system for this did not decrease the amplitude of the peak at this frequency. Our next hypothesis was that the lack of performance by the controller was because the amplitude of response measured from the piezoelectric sensor during lathing was an order of magnitude smaller than that measured by the sensor during lab random noise and impact tests.

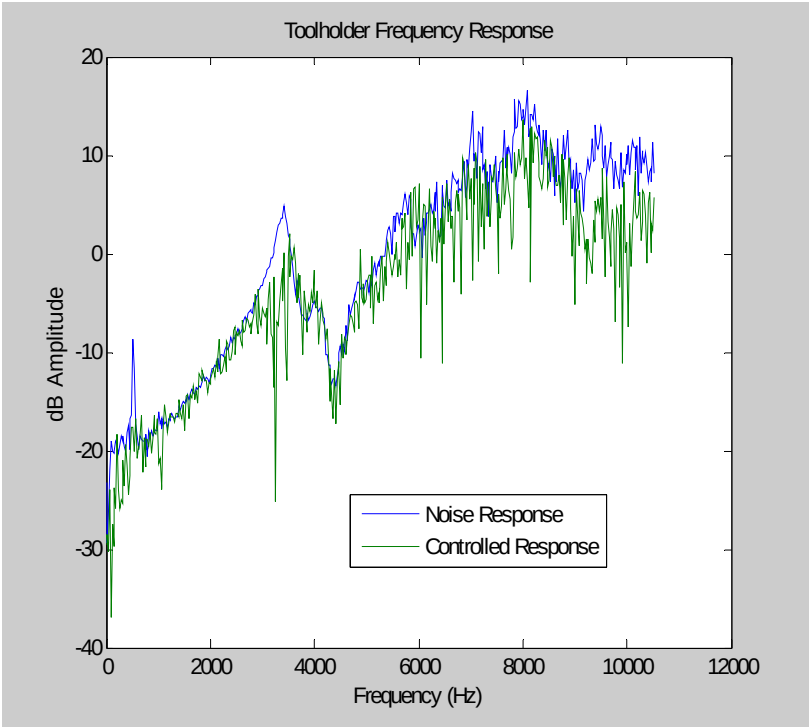

Figure 11: Frequency Performance of Controller

Turning tests were redone while sending a small amplitude random noise signal to the actuator. A low pass filter was included to roll the frequency off from 5000 to 7000 Hz. Frequency analysis of the sensor showed that the noise significantly increased the signal strength picked up from the sensor. Figure 11 shows the frequency response of the sensor signal while taking a 0.004 in deep cut with 1200 rpm spindle speed with 0.005 in/rev feed rate on the aluminum bar stock. Tuning the controller for the 3700 Hz frequency caused a decrease of over 5 dB for the 3700 Hz peak and completely eliminated the 515 Hz chatter frequency. Surface finish improvement was dramatic. The uncontrolled cut yielded a roughness average of 71.6 uin while the controlled cut yielded an average of 40.5 uin.

The small noise signal increased the signal strength and frequency bandwidth enough for the controller to engage and perform in a stable manor. Tests taken at several different combinations of cut depth and spindle speed showed an average roughness increase of 2 uin from the noise signal. This negative effect is nullified when the controller is performing however because of how much the controller decreases the 515 Hz chatter resonance.

Differing cut depths were taken in order to characterize the performance range of the cutter and controller. Figure 12 shows a plot of surface roughness of cuts taken at different depths with a 200v amplifier and 1000v amplifier against baseline uncontrolled tests. The results show significant improvement for radial cut depths of 0.002 in to 0.015 in. Performance was limited to 0.010 uin for the 200v amplifier because deeper cuts caused its output to become saturated because it could not apply the voltage required to get the necessary tool displacement. Slight performance degradation at 0.001 uin is most likely attributed to the smallness of the chatter response signal. Performance benefits cut off after 0.015 uin because the displacement of the cutter is limited to around 2 um or 80 uin which is equal to the displacement of the chatter for an uncontrolled cut at 0.015 in cut depth. When the chatter displacement exceeds the max displacement of the toolholder the controller becomes completely ineffective. All tests for Figure 12 were done after the controller had been tuned for 0.004 in cut depth. This proved the controllers robustness. Baseline tests determined that the spindle speed would need to

be decreased by about 50% to approximately 600 rpm in order to achieve similar surface finish quality as was achieved with the controlled tests. This showed that the controlled toolholder possibly allows a machinist to double spindle speed on chatter limited cuts. This could have significant cost savings in machine shops which machine complex parts with low stiffness.

Previous cuts were all done on 1.5in to 2in shafts with pre-existing 40uin surface roughness. The active vibration toolholder was capable of matching this surface finish at higher spindle speeds where chatter typically exists. Further tests were done with shafts with pre-existing surface finish chatter. Because the PPF controller tries to damp out variations in force between the cutter and workpiece the controller basically maps the pre-existing chatter to the cutter to equalize cutting force thereby maintaining the poor surface finish on the subsequent cut. This is a drawback to the simple PPF controller but does not hurt its application. If a shaft of poor surface finish needs to be turned down it can first be cleaned up with a slow chatter free cut with the controller off. Once the desired surface finish is cut then the controller can be turned on and the spindle speed can be significantly increased to hog off material. This means the adaptive vibration reduction toolholder has applications to both roughing and finish cut operations.

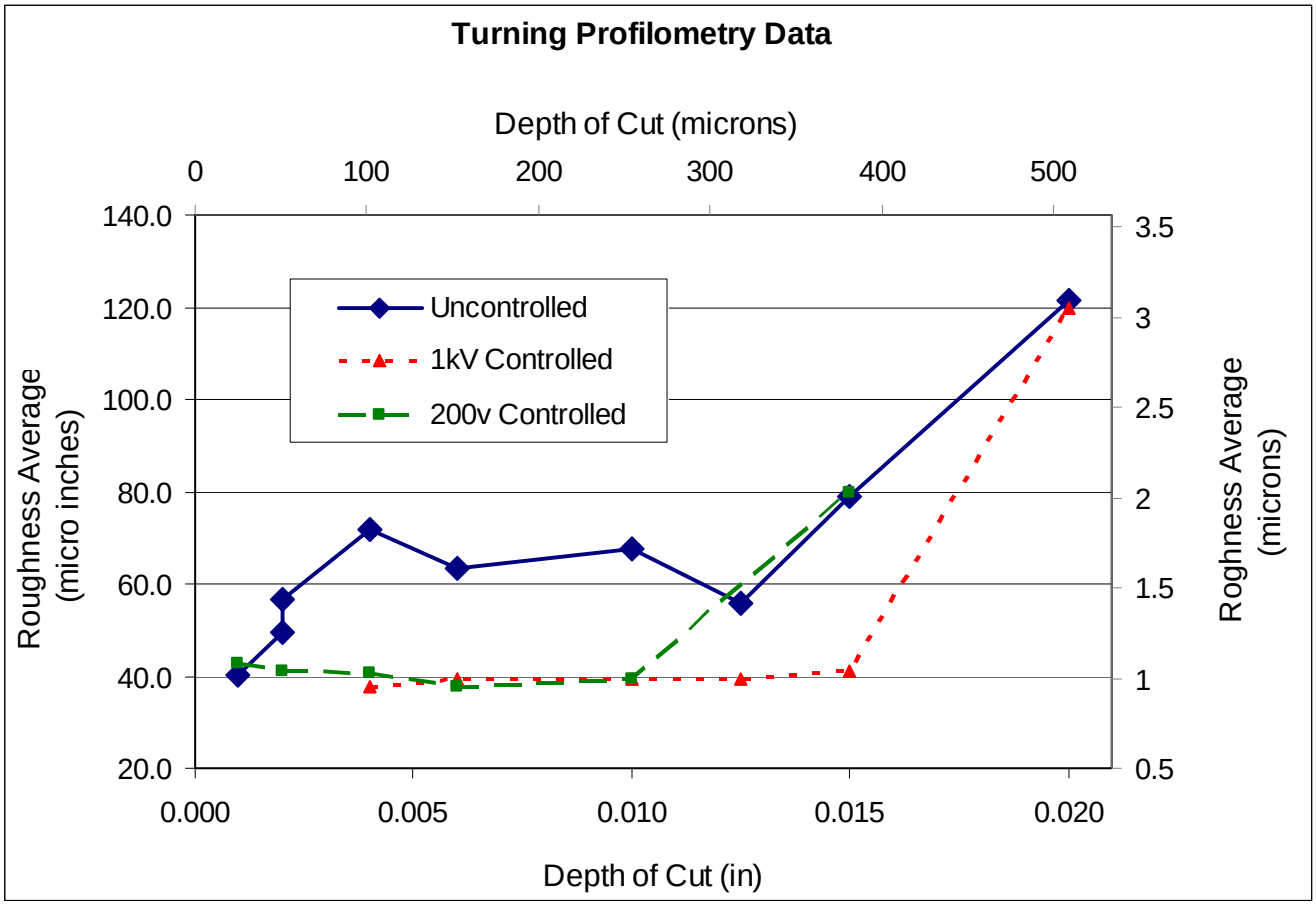

Figure 12: Surface Roughness Performance (1200rpm, 0.005 in/rev feed)

4 CONCLUSION

An active vibration control toolholder for lathe machining reduces chatter and significantly increases surface finish quality for chatter limited turning operations. It allows for doubling spindle speeds while keeping equivalent surface finish provided the tool holder displacement is capable of matching the chatter peak to peak magnitude. The toolholder permits reliable machining of less stiff workpieces with low cost hardware and a relatively simple control system. Demonstration of the toolholder proved its cost effective application to standard lathe operations and possible application to specialty lathe operations.

Future work needs to be done to investigate the application of this toolholder's performance and the controller's performance to plutonium manufacturing. Tests need to be run on facing operations and the contour mapping problem of turning rough workpieces needs to be further investigated for alternative solutions.

5 ACKNOWLEDGEMENTS

Funding for this research was provided by the Department of Energy through the Los Alamos National Laboratory. The following companies generously provided various software packages to aid in modeling and data analysis: Vibrant Technologies, SIMULIA, and The Mathworks. Finally, the authors would like to thank Dr. Charles Farrar and the Los Alamos Dynamics Summer School for the opportunity to conduct this research.

6 REFERENCES

[1] Kalpakjian, S., Schmid, S.R.. (2008). *Manufacturing Processes for Engineering Matrials* (5th ed.). Upper Saddle River, NJ: Pearson Education, Inc.

[2] Park, G., Bement, M. T., Hartman, D. A., Smith, R. E., & Farrar, C. R. (2007). The use of active materials for machining processes: A review. *Interantional Journal of Machine Tools and Manufacture , 47*, 2189-2206.

[3] Babitsky, V. I., Kalashnikov, A. N., Meadows, A., & Wijesundara, A. (2003). Ultrasonically assisted turning of aviation materials. *Journal of Materials Processing Technology , 132*, 157-167.

[4] Chang, S. S., & Bone, G. M. (2005). Burr size reduction indrilling by ultrasonic assistance. *Robotics and Computer-Integrated Manufacturing , 21*, 21.

[5] Amini, S., Soleimanimehr, H., Nategh, M. J., Abudollah, A., & Sadeghi, M. H. (2008). FEM analysis of ultrasonic-vibration-assisted turning and the vibratory tool. *Journal of Materials Processing and Technology , 201*, 43-47.

[6] Mitrofanov, A. V., Babitsky, V. I., & Silberschmidt, V. V. (2005). Thermomechanical finite element simulations of ultrasonically assisted turning. *Computational Materials Science , 32*, 463-471.

[7] Thoe, T., Aspinwall, D., & Wise, M. (1998). Review on Ultrasonic Machining. *38* (4), 239-255.

[8]Wang, J., & Su, C.-Y. (2003). Two degree-of-freedom modeling and robust chatter control in metal cutting by piezoelectricity. *Proceedings of the American Control Conference* (pp. 3044-3048). Denver, CO: IEEE.

[9] Mei, C. (2005). Active regenerative chatter suppression during boring manufacturing process. *Robotics and Computer-Integrated Manufacturing , 21*, 153-158.

[10] Espinoza, A. A., Mayer, L. J., Oberlin, P. V., & Bement, M. (2006, August). *Design and evaluation of a piezoelectric actuator for turning.* Retrieved June 18, 2008, from Los Alamos National Labs: Engineering Institute: LADSS: http://www.lanl.gov/projects/ei/DSS/projects/2006/Bement/design%20and%20evaluation_paper

.pdf
[11] Creasy, M., Leo, D., & Farinholt, K. (2008). Adaptive positive position feedback for actively absorbing energy in acoustic cavities. *Journal of Sound and Vibration , 311*, 461-472.
[12] Bilinear transform. (2008, May 6). In *Wikipedia, The Free Encyclopedia*. Retrieved 06:13, August 8, 2008, from http://en.wikipedia.org/w/index.php?title=Bilinear_transform&oldid=210516649